Supplementary Material: The long–term sea–level commitment from Antarctica

Ann Kristin Klose[1,2], Violaine Coulon[3], Frank Pattyn[3], and Ricarda Winkelmann[1,2]

[1]FutureLab Earth Resilience in the Anthropocene, Earth System Analysis & Complexity Science, Potsdam Institute for Climate Impact Research (PIK), Member of the Leibniz Association, 14473 Potsdam, Germany
[2]Institute of Physics and Astronomy, University of Potsdam, 14476 Potsdam, Germany
[3]Laboratoire de Glaciologie, Université libre de Bruxelles (ULB), Brussels, Belgium

Correspondence: Ann Kristin Klose (annkristin.klose@pik-potsdam.de) and Ricarda Winkelmann (ricarda.winkelmann@pik-potsdam.de)

Table S1. Projected atmospheric temperature change at different points in time. Projected Antarctic–averaged atmospheric temperature change with respect to mean over time period 1995–2014 at different points in time for the four CMIP6 GCMs used to force the ice–sheet models. For a given point in time, upper rows represent SSP1-2.6 and lower rows correspond to SSP5-8.5.

		MRI-ESM2-0	CESM2-WACCM	IPSL-CM6A-LR	UKESM1-0-LL
2050	SSP1-2.6	0.90	1.26	1.54	1.34
	SSP5-8.5	1.38	1.90	1.85	1.86
2100	SSP1-2.6	1.38	2.43	1.56	1.26
	SSP5-8.5	5.02	6.35	5.30	6.20
2150	SSP1-2.6	1.77	2.50	1.10	1.35
	SSP5-8.5	8.50	10.47	8.99	9.66
2200	SSP1-2.6	1.89	2.86	1.16	1.39
	SSP5-8.5	10.70	13.36	11.67	11.80
2250	SSP1-2.6	2.26	2.81	1.44	1.18
	SSP5-8.5	11.57	15.14	13.39	13.05
2300	SSP1-2.6	2.36	3.58	0.98	1.22
	SSP5-8.5	12.14	16.4	14.08	13.52

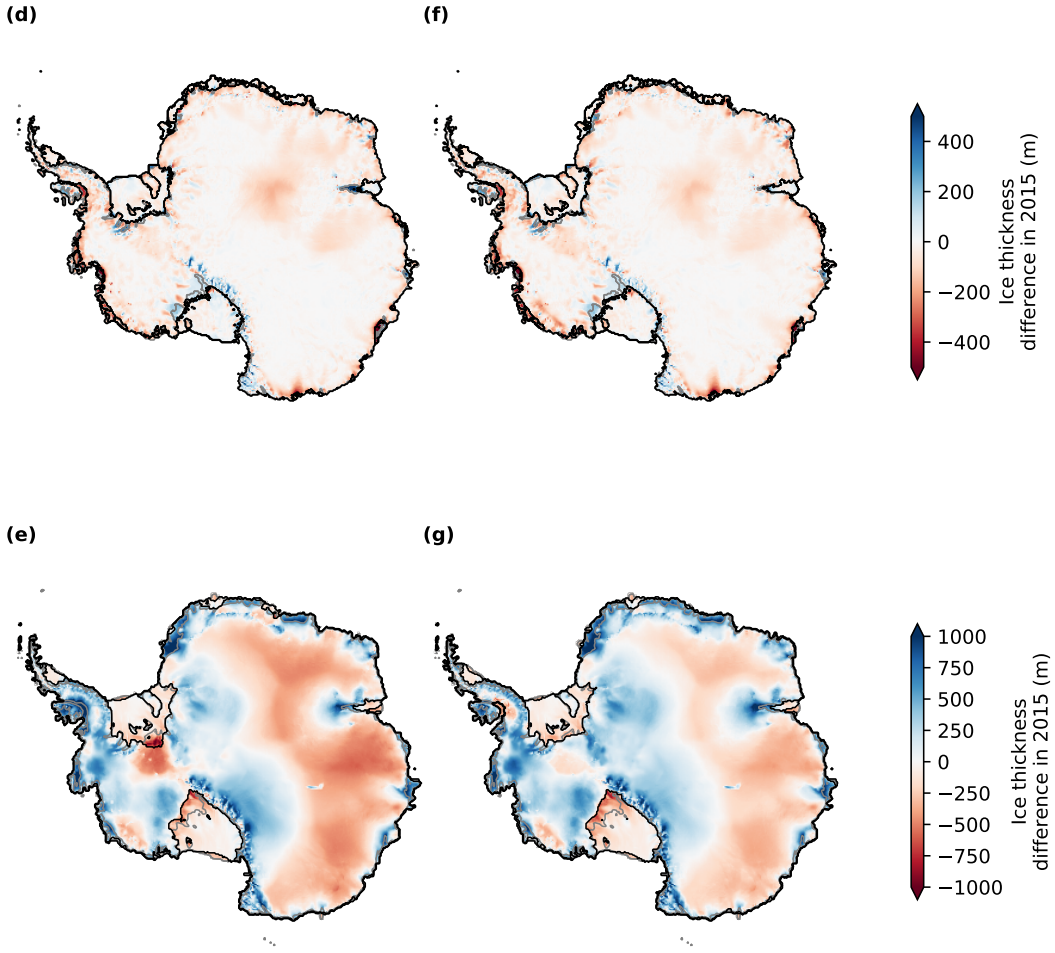

Figure S1. Comparison between modelled and observed ice–sheet geometry. Modelled present–day ice thickness in Kori-ULB (upper row) and PISM (lower row), using atmospheric climatologies based on MAR (left column) and RACMO (right column) relative to observed ice thickness (Bedmachine for Kori-ULB and Bedmap2 for PISM). Modelled and observed grounding line and calving front position are shown in black and grey, respectively. Note the different scales of the colourbar for Kori-ULB and PISM.

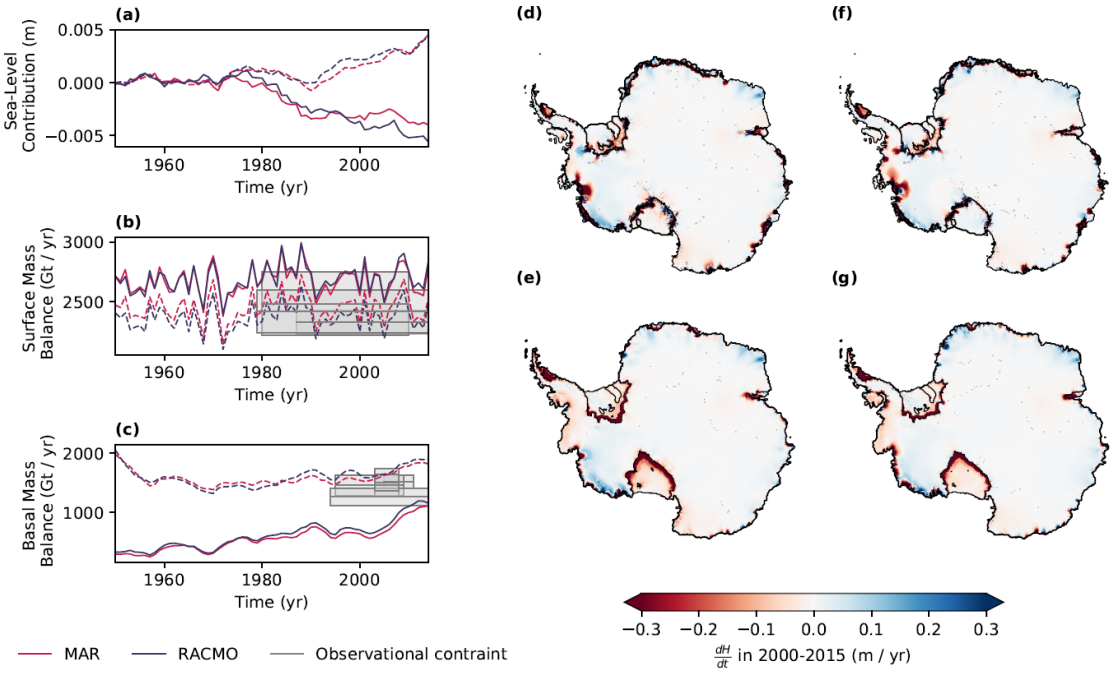

Figure S2. Trajectories of the Antarctic Ice Sheet over the historical period Evolution of the ice sheet from 1950 to 2015 as determined by the ice–sheet models Kori-ULB (dashed) and PISM (solid) in terms of (a): Sea–level contribution (based on volume above floatation), (b): Surface mass balance, and (c): Sub–shelf melt. (d)–(g): Rate of ice thickness change from 2000 to 2015 as determined by Kori-ULB (upper row) and PISM (lower row), using atmospheric climatologies based on MAR (left column) and RACMO (right column). Observations of the ice–sheet mass balance components (as in Coulon et al., 2023) are given by grey boxes (indicating the time period and uncertainties of the respective observation), where the solid line shows the mean.

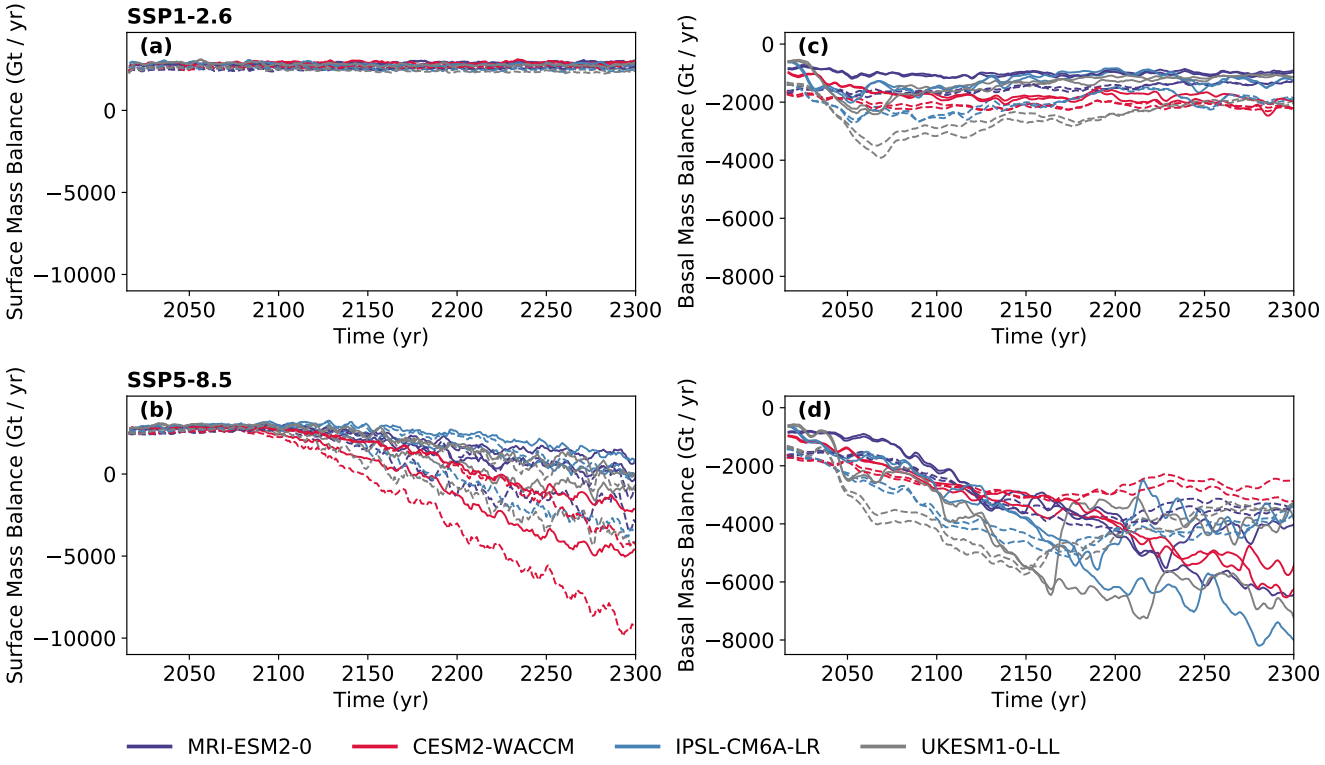

Figure S3. Projected trajectories of the Antarctic Ice Sheet in response to changing climate conditions as projected by four different GCMs (given by the colour) under emission pathways SSP1-2.6 (upper row) and SSP5-8.5 (lower row), as determined by the ice–sheet models Kori-ULB (dashed) and PISM (solid) in terms of (a) and (b): Surface mass balance, and (c) and (d): Sub–shelf melt.

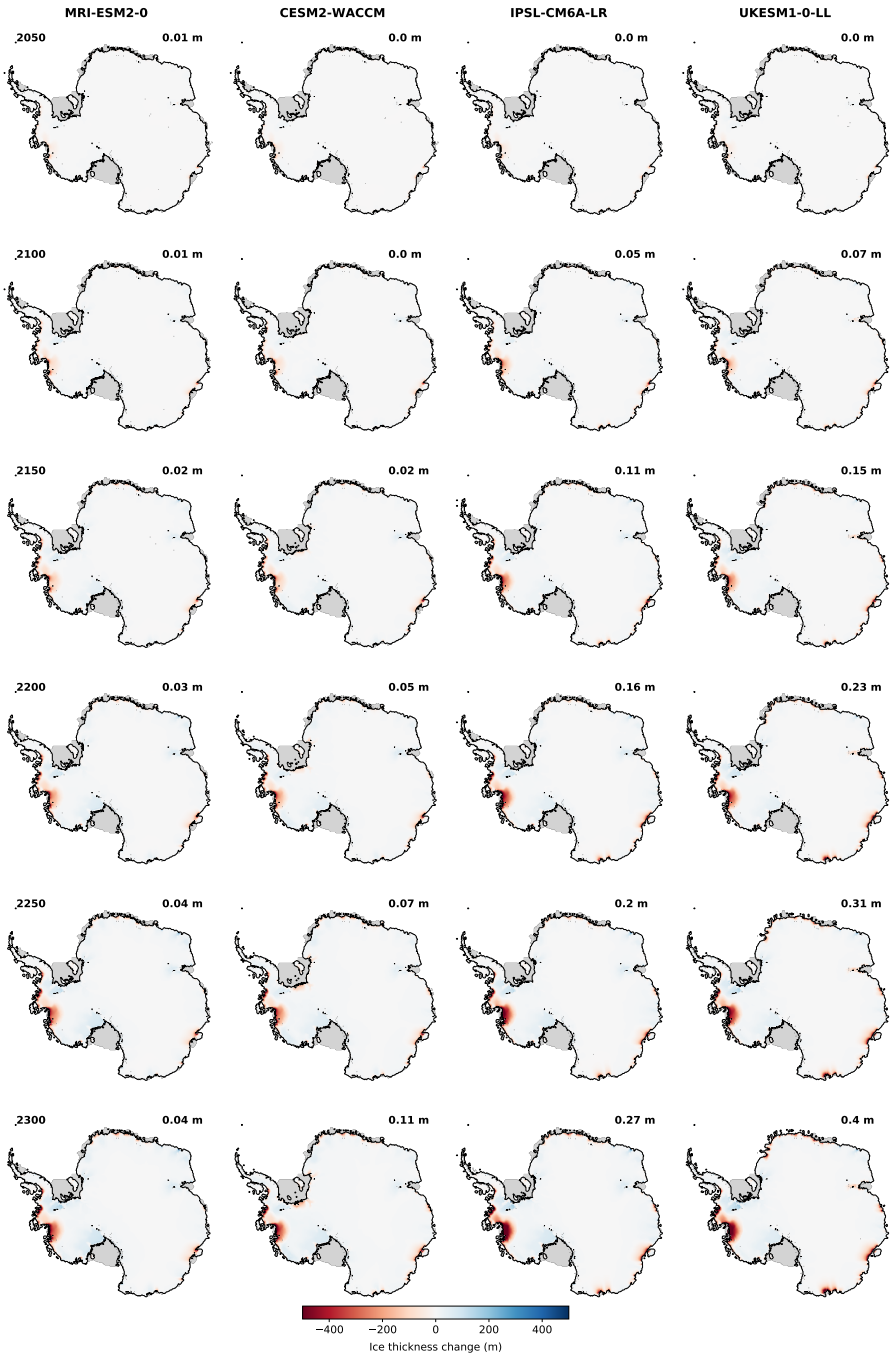

Figure S4. Transient ice–sheet evolution as determined by Kori-ULB following the lower–emission pathway SSP1-2.6 and using an atmospheric climatology based on MAR. Shown is the transient thickness change and grounding–line location (marked in black) in response to climatic boundary conditions as projected by CMIP6 GCMs. Ice shelves are indicated in light grey.

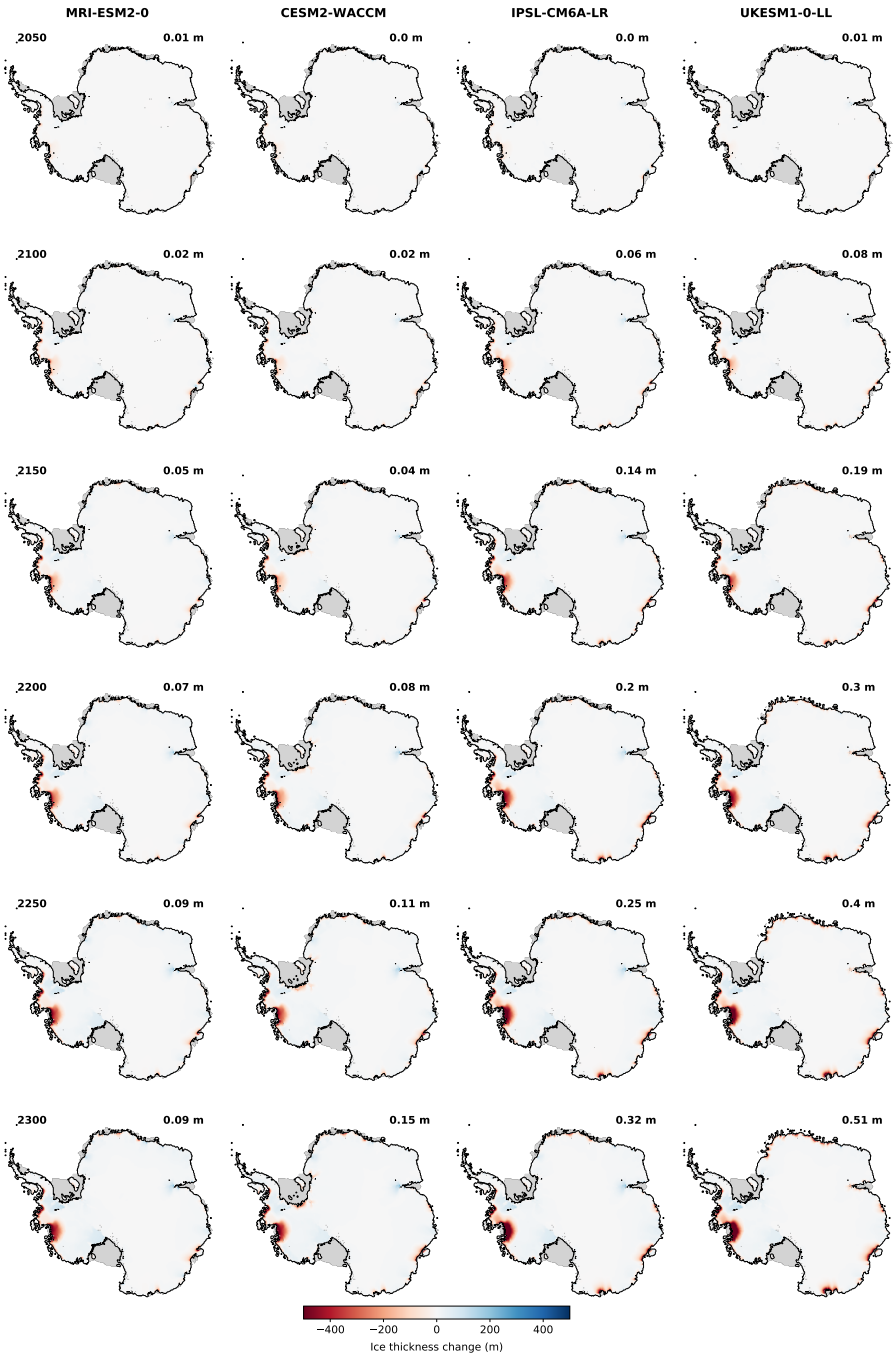

Figure S5. Transient ice–sheet evolution as determined by Kori-ULB following the lower–emission pathway SSP1-2.6 and using an atmospheric climatology based on RACMO. Shown is the transient thickness change and grounding–line location (marked in black) in response to climatic boundary conditions as projected by CMIP6 GCMs.Ice shelves are indicated in light grey.

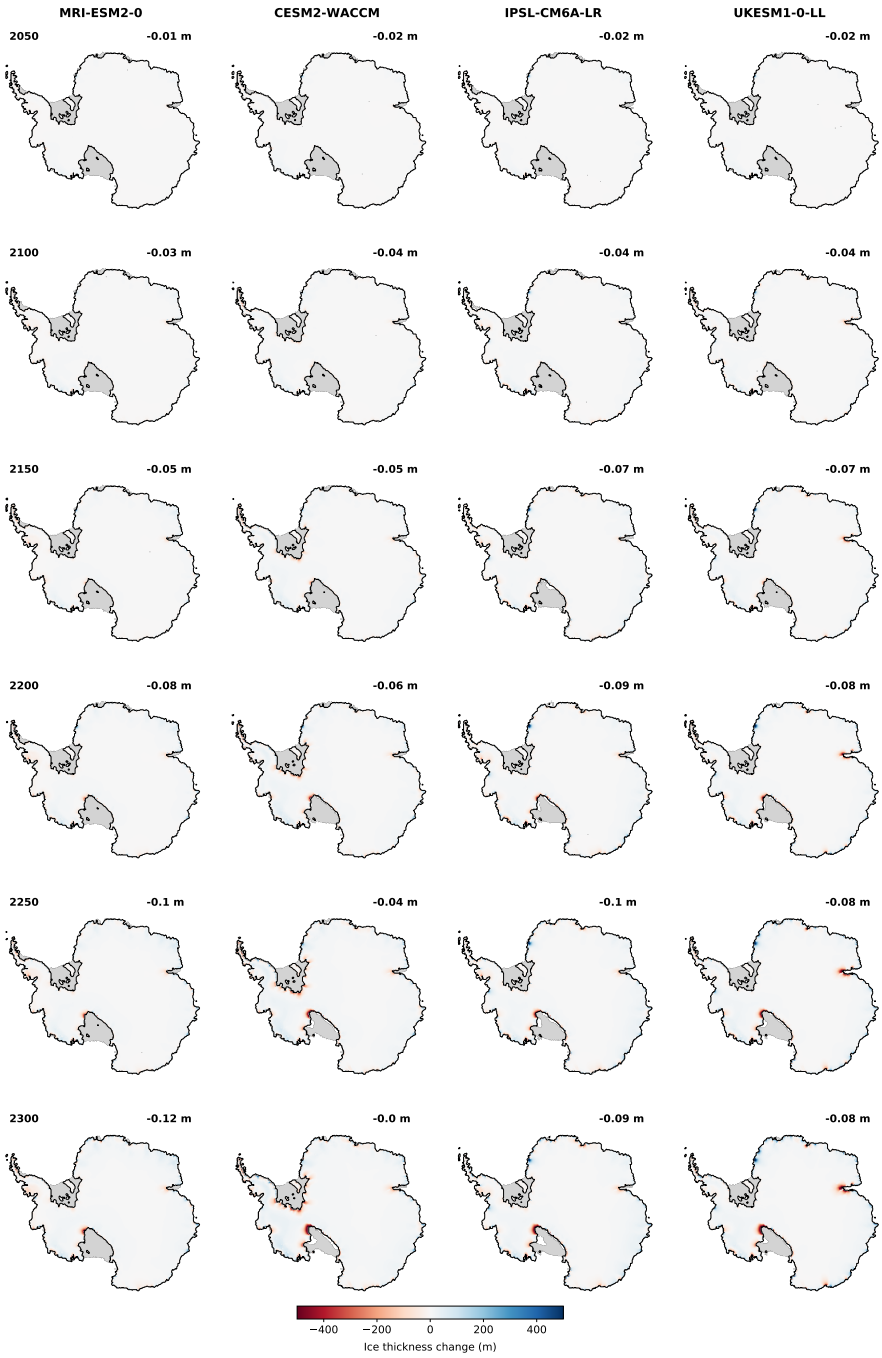

Figure S6. Transient ice–sheet evolution as determined by PISM following the lower–emission pathway SSP1-2.6 and using an atmospheric climatology based on MAR. Shown is the transient thickness change and grounding–line location (marked in black) in response to climatic boundary conditions as projected by CMIP6 GCMs. Ice shelves are indicated in light grey.

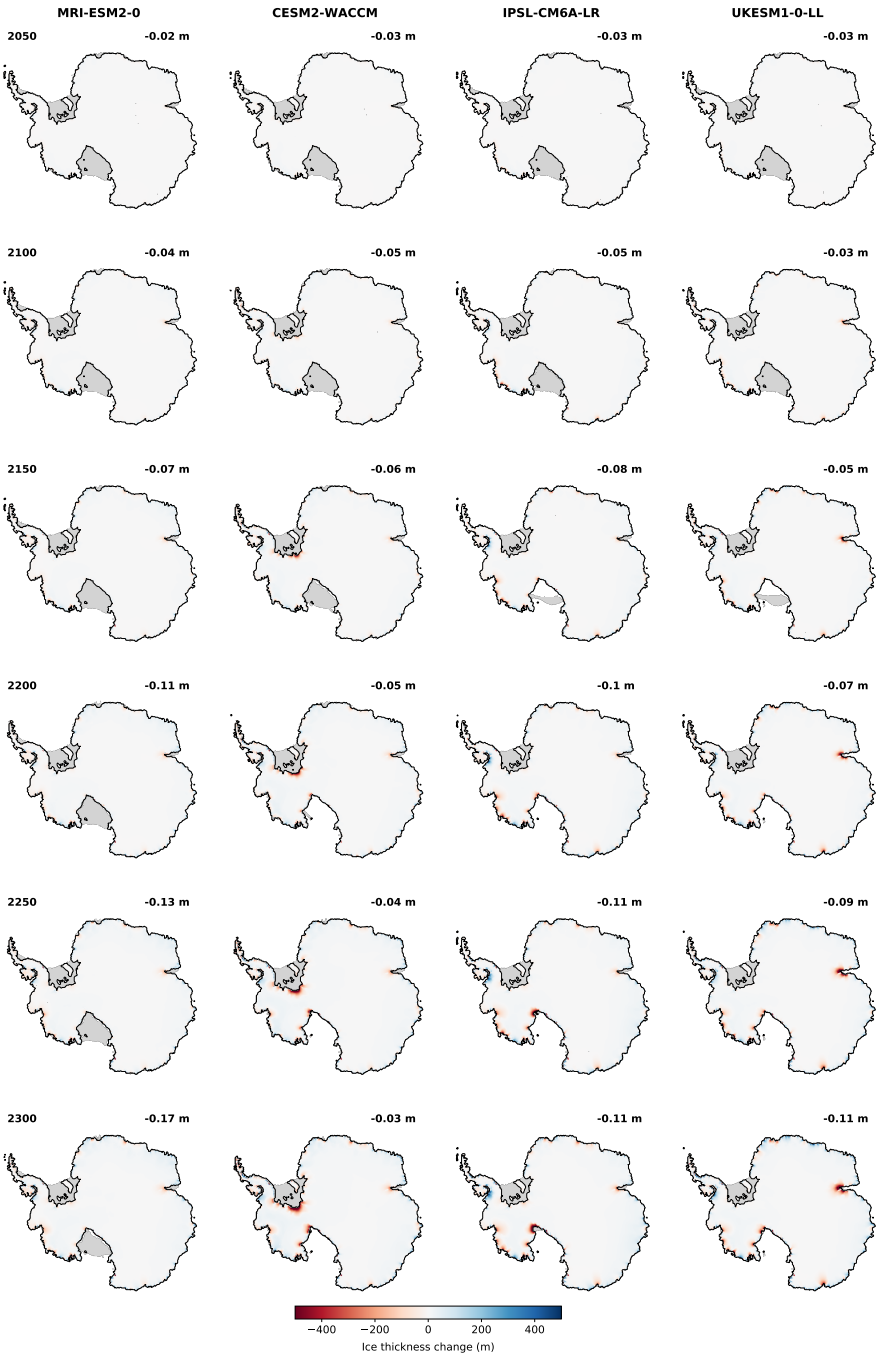

Figure S7. Transient ice–sheet evolution as determined by PISM following the lower–emission pathway SSP1-2.6 and using an atmospheric climatology based on RACMO. Shown is the transient thickness change and grounding–line location (marked in black) in response to climatic boundary conditions as projected by CMIP6 GCMs. Ice shelves are indicated in light grey.

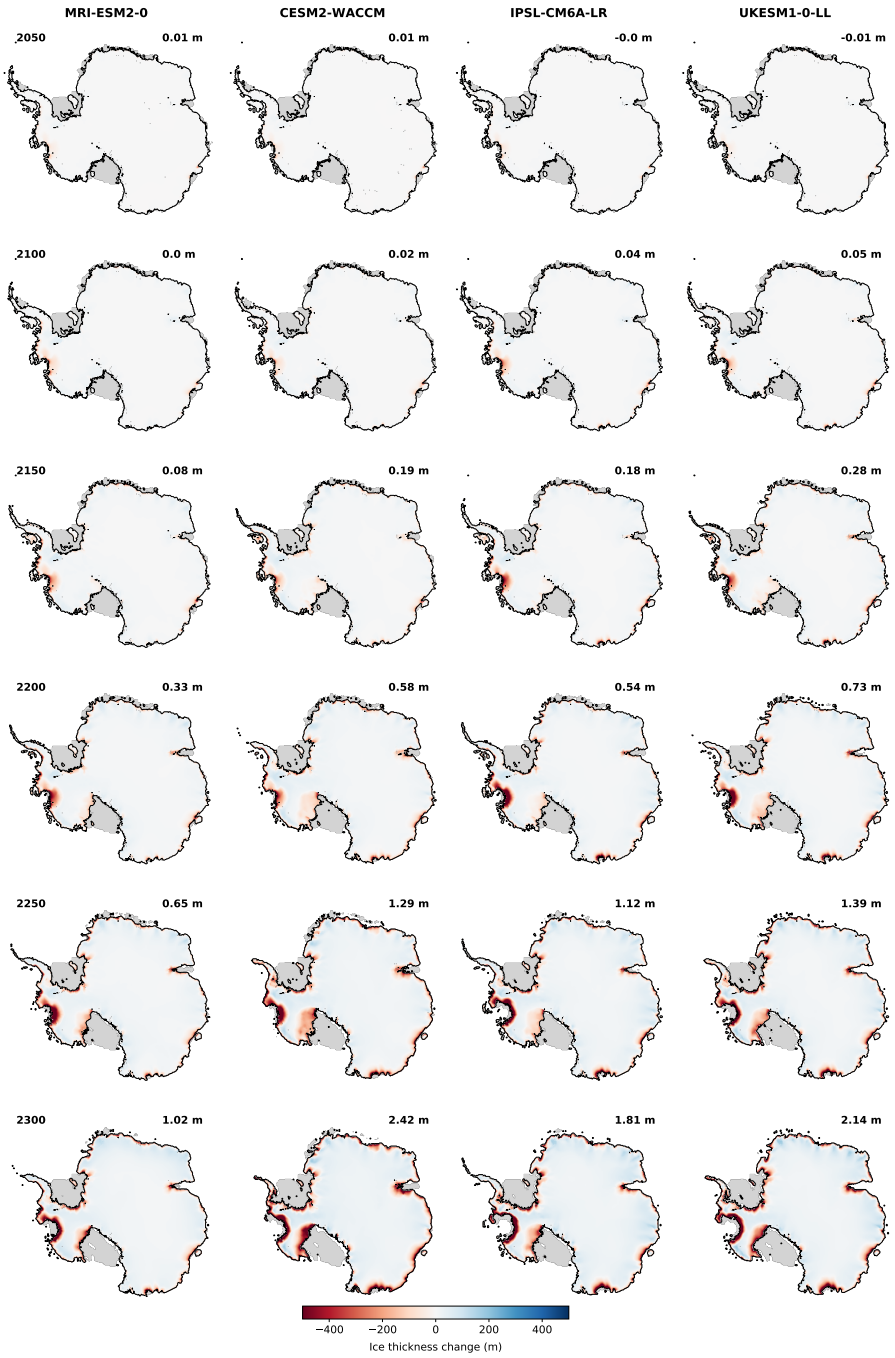

Figure S8. Transient ice–sheet evolution as determined by Kori-ULB following the higher–emission pathway SSP5-8.5 and using an atmospheric climatology based on MAR. Shown is the transient thickness change and grounding–line location (marked in black) in response to climatic boundary conditions as projected by CMIP6 GCMs. Ice shelves are indicated in light grey.

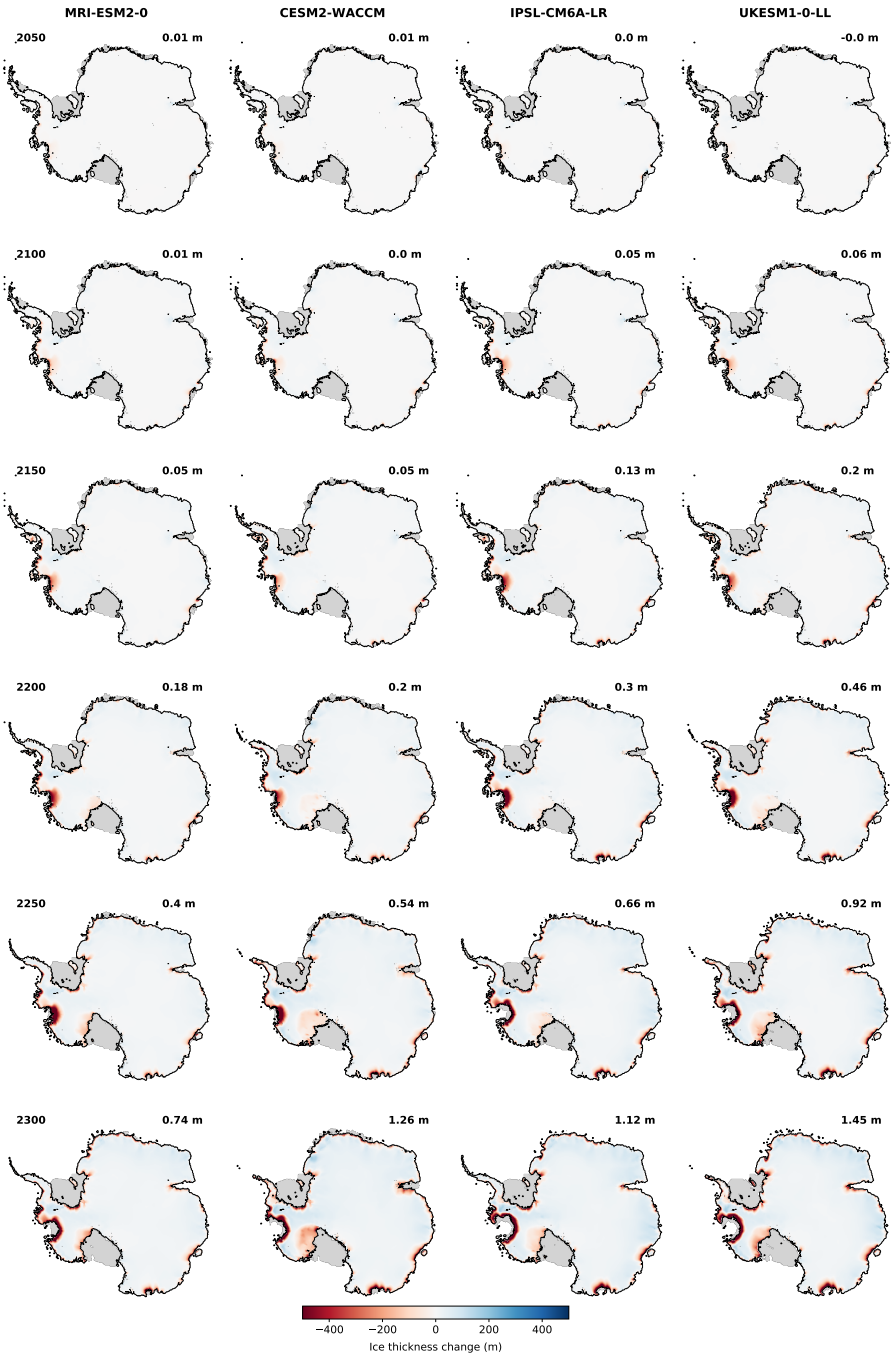

Figure S9. Transient ice–sheet evolution as determined by Kori-ULB following the higher–emission pathway SSP5-8.5 and using an atmospheric climatology based on RACMO. Shown is the transient thickness change and grounding–line location (marked in black) in response to climatic boundary conditions as projected by CMIP6 GCMs. Ice shelves are indicated in light grey.

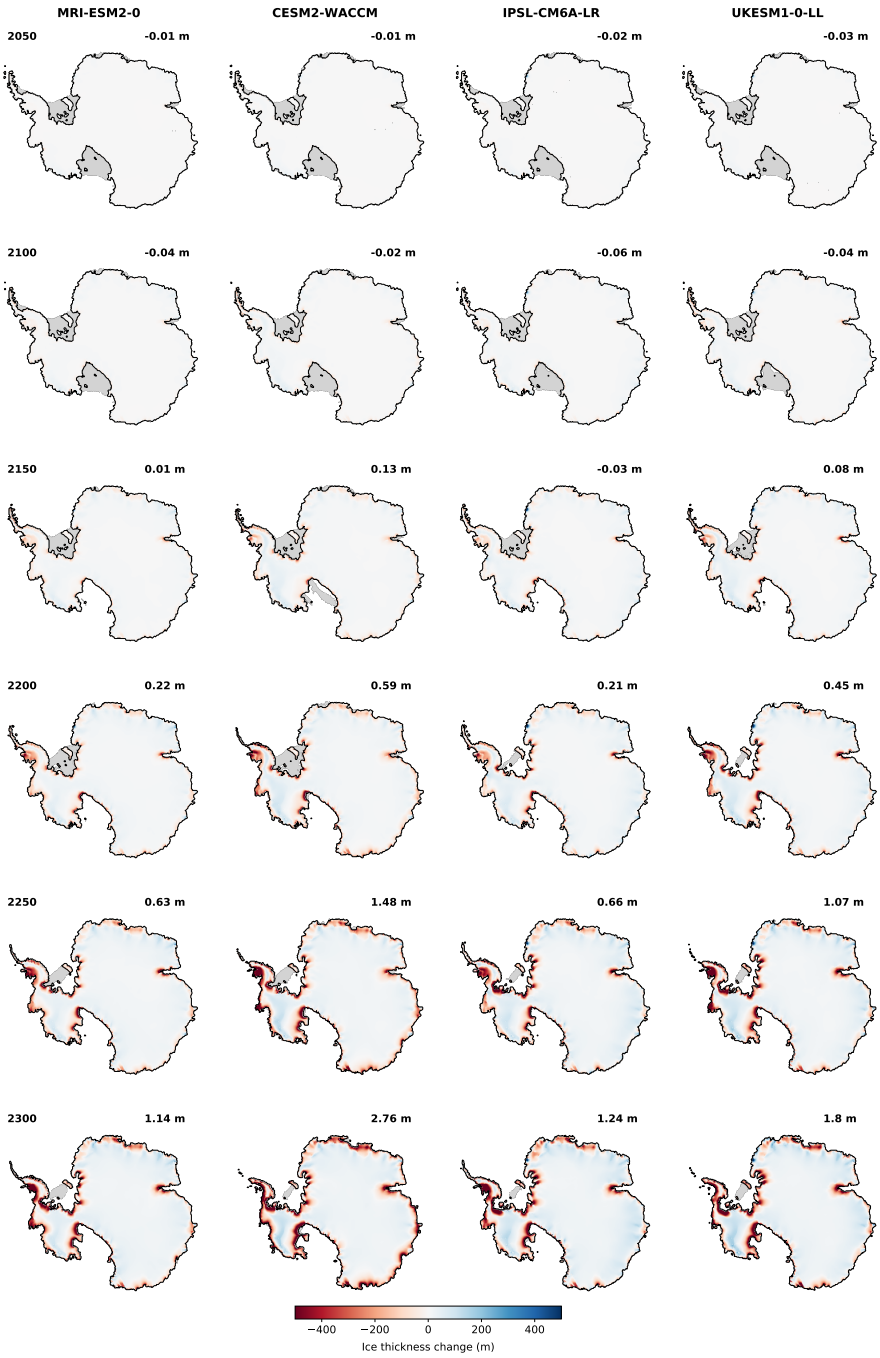

Figure S10. Transient ice–sheet evolution as determined by PISM following the higher–emission pathway SSP5-8.5 and using an atmospheric climatology based on MAR. Shown is the transient thickness change and grounding–line location (marked in black) in response to climatic boundary conditions as projected by CMIP6 GCMs. Ice shelves are indicated in light grey.

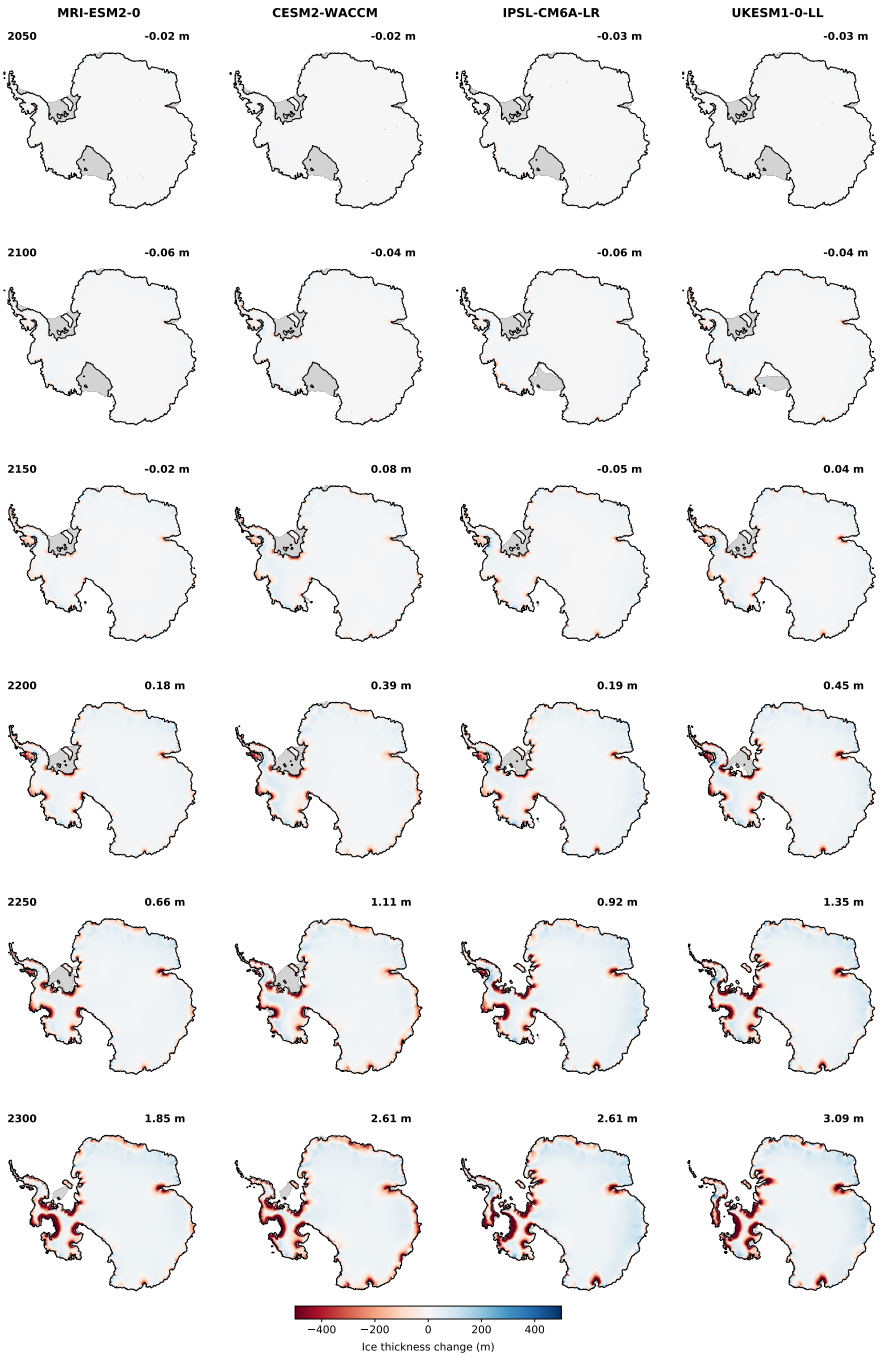

Figure S11. Transient ice–sheet evolution as determined by PISM following the higher–emission pathway SSP5-8.5 and using an atmospheric climatology based on RACMO. Shown is the transient thickness change and grounding–line location (marked in black) in response to climatic boundary conditions as projected by CMIP6 GCMs. Ice shelves are indicated in light grey.

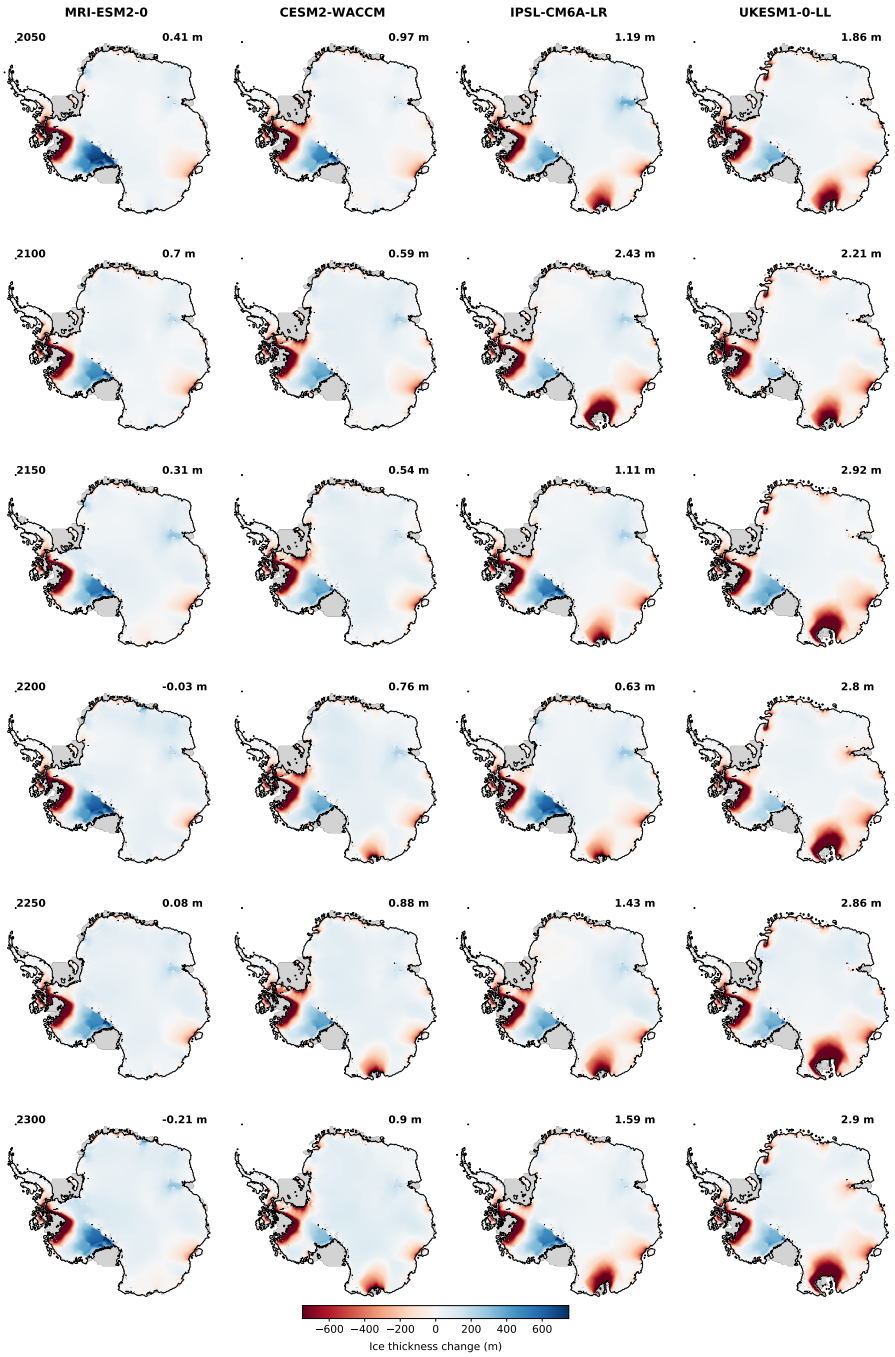

Figure S12. Committed ice–sheet configuration as determined by Kori-ULB following the lower–emission pathway SSP1-2.6 and using an atmospheric climatology based on MAR. Shown is the committed thickness change and grounding–line location (marked in black) in year 7000 when stabilising climatic boundary conditions as projected by CMIP6 GCMs at different points in time. Ice shelves are indicated in light grey.

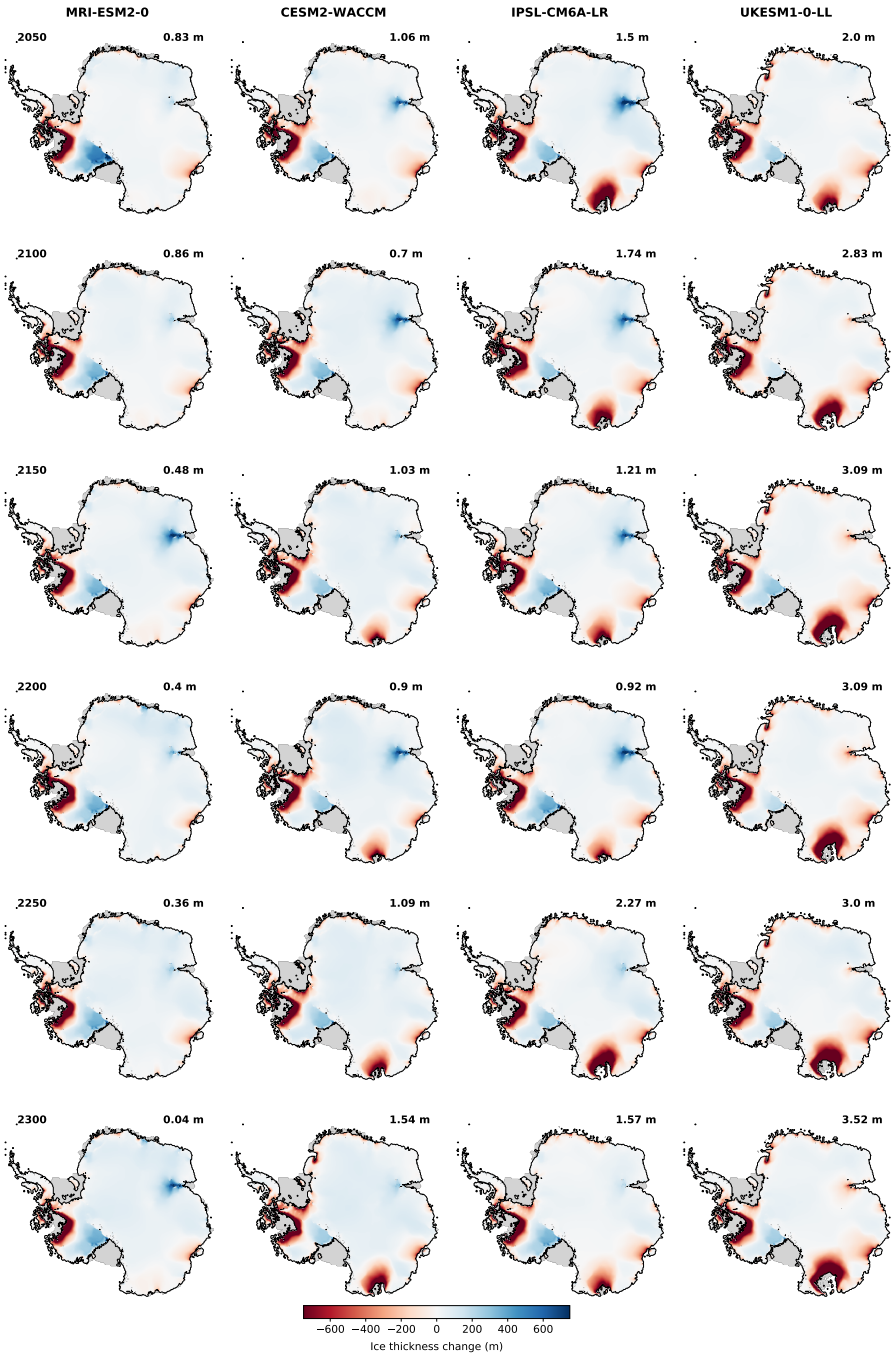

Figure S13. Committed ice–sheet configuration as determined by Kori-ULB following the lower–emission pathway SSP1-2.6 and using an atmospheric climatology based on RACMO. Shown is the committed thickness change and grounding–line location (marked in black) in year 7000 when stabilising climatic boundary conditions as projected by CMIP6 GCMs at different points in time. Ice shelves are indicated in light grey.

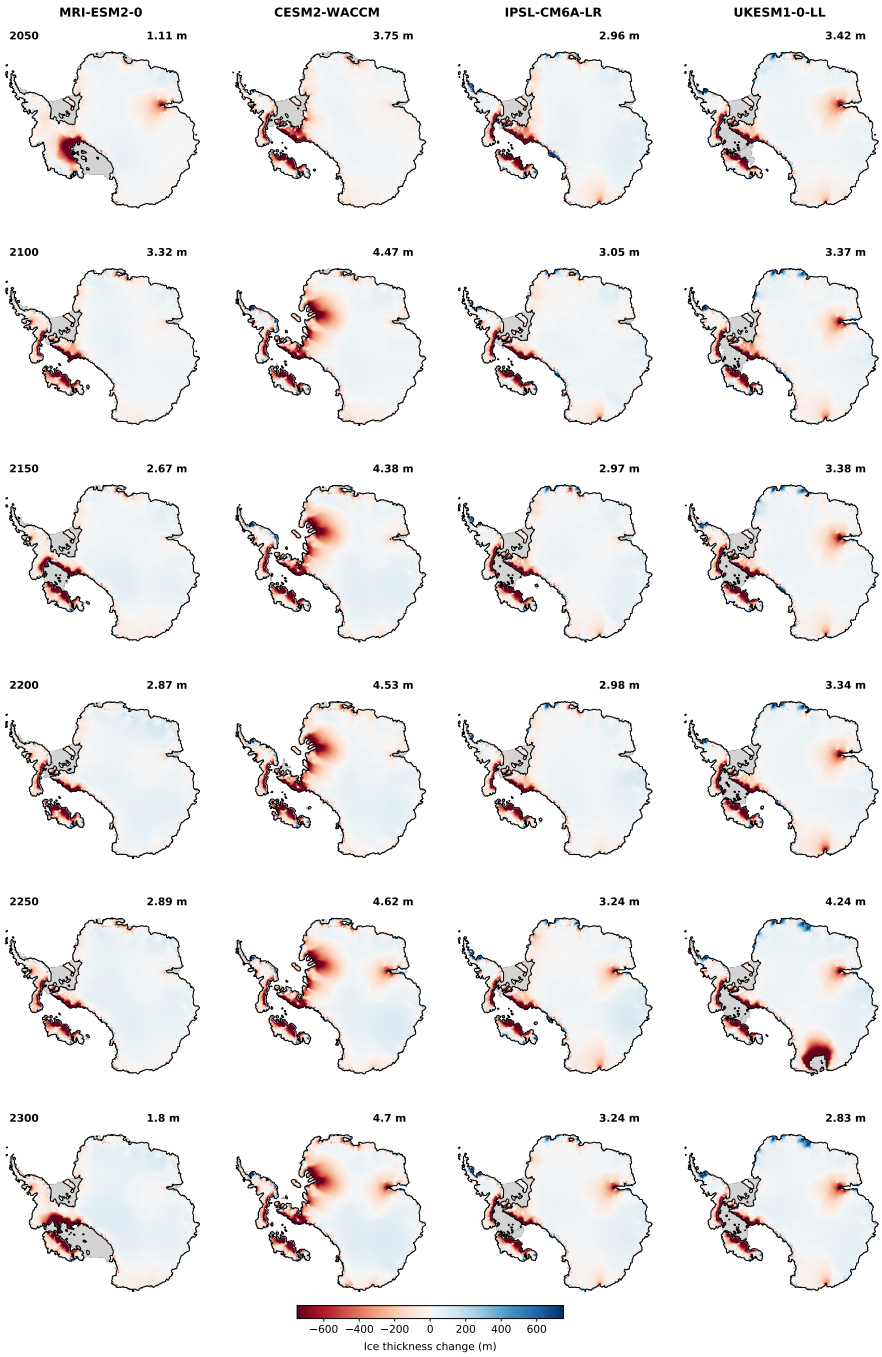

Figure S14. Committed ice–sheet configuration as determined by PISM following the lower–emission pathway SSP1-2.6 and using an atmospheric climatology based on MAR. Shown is the committed thickness change and grounding–line location (marked in black) in year 7000 when stabilising climatic boundary conditions as projected by CMIP6 GCMs at different points in time. Ice shelves are indicated in light grey.

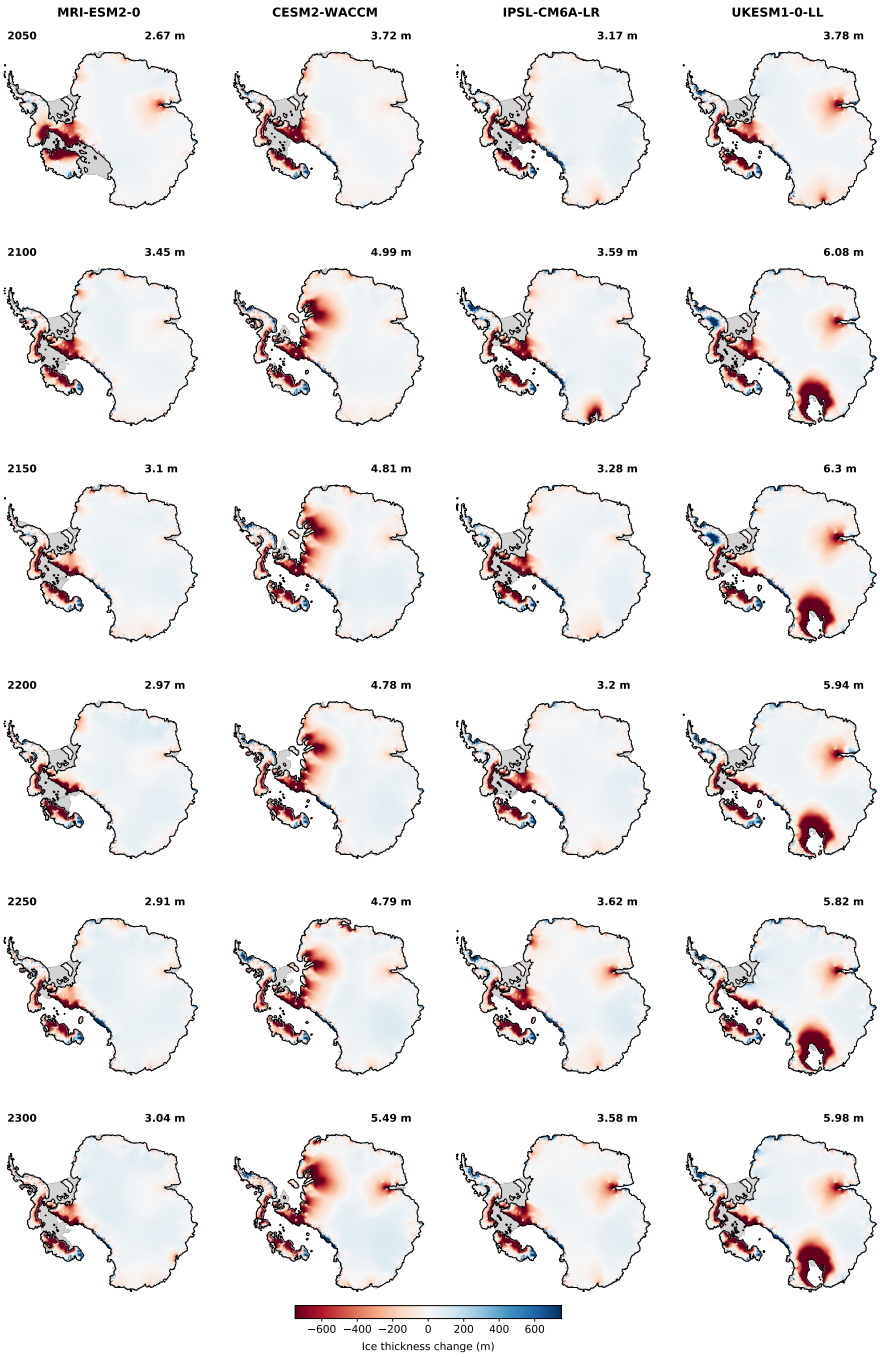

Figure S15. Committed ice–sheet configuration as determined by PISM following the lower–emission pathway SSP1-2.6 and using an atmospheric climatology based on RACMO. Shown is the committed thickness change and grounding–line location (marked in black) in year 7000 when stabilising climatic boundary conditions as projected by CMIP6 GCMs at different points in time. Ice shelves are indicated in light grey.

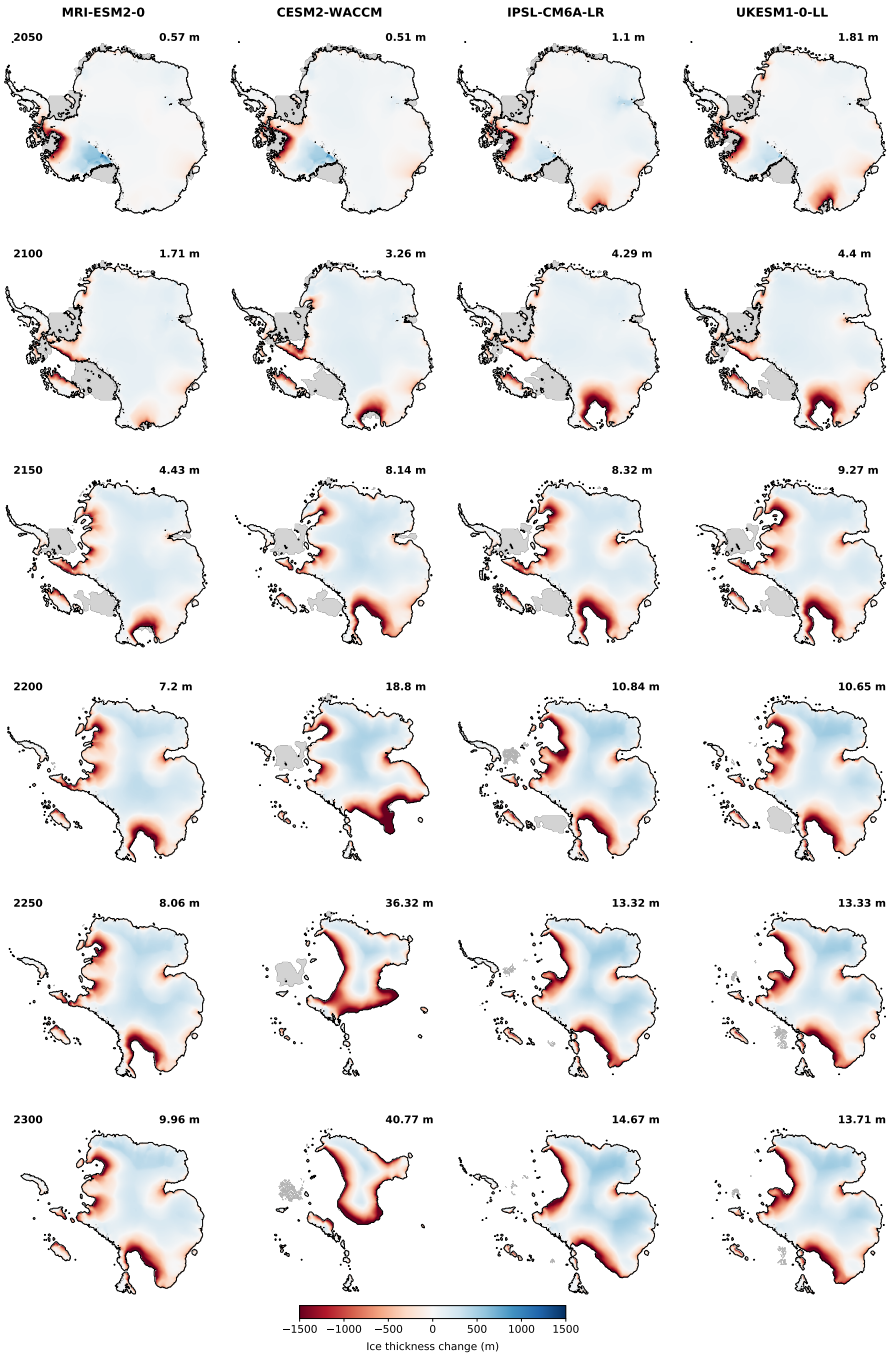

Figure S16. Committed ice–sheet configuration as determined by Kori-ULB following the higher–emission pathway SSP5-8.5 and using an atmospheric climatology based on MAR. Shown is the committed thickness change and grounding–line location (marked in black) in year 7000 when stabilising climatic boundary conditions as projected by CMIP6 GCMs at different points in time. Ice shelves are indicated in light grey.

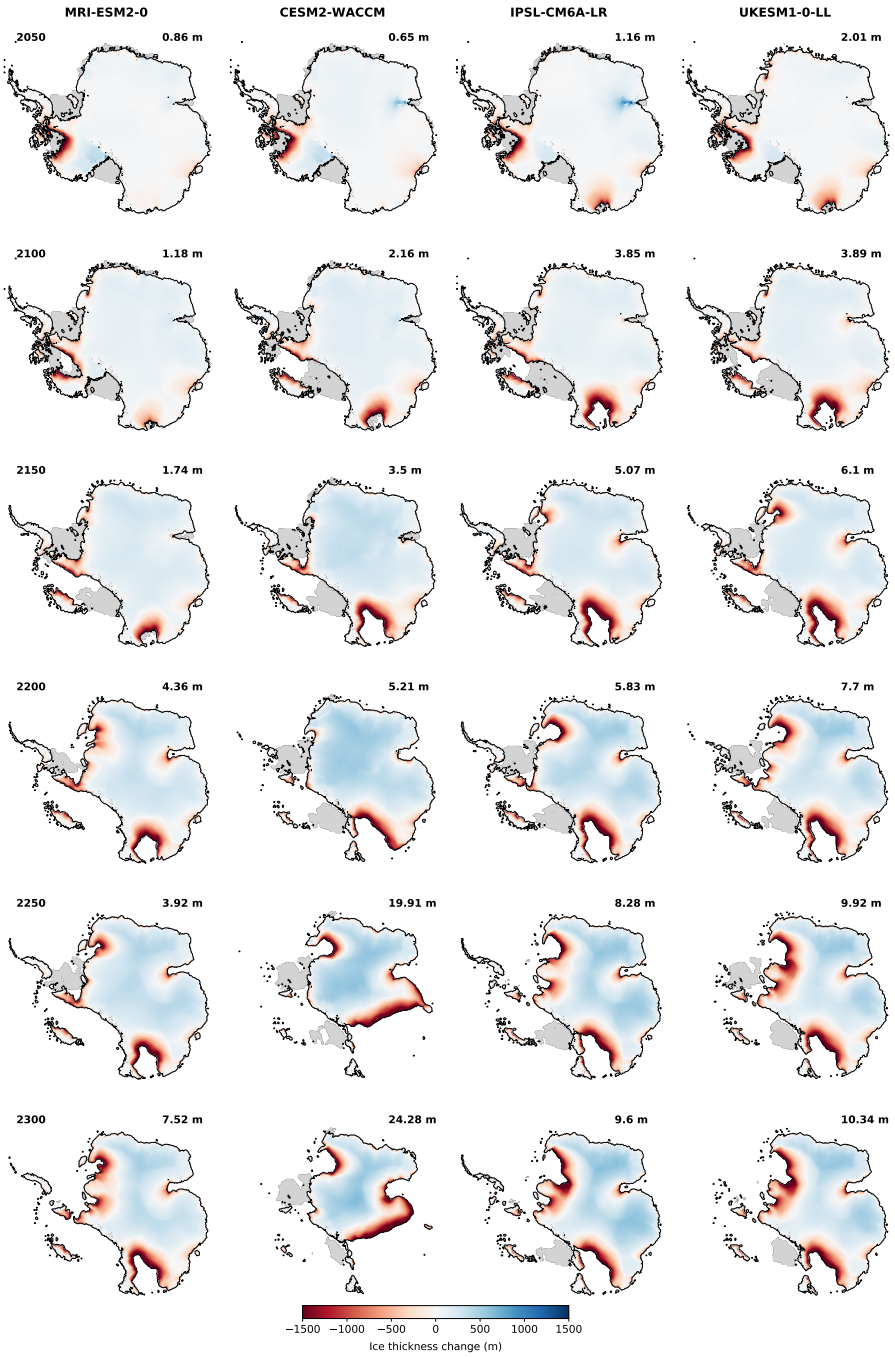

Figure S17. Committed ice–sheet configuration as determined by Kori-ULB following the higher–emission pathway SSP5-8.5 and using an atmospheric climatology based on RACMO. Shown is the committed thickness change and grounding–line location (marked in black) in year 7000 when stabilising climatic boundary conditions as projected by CMIP6 GCMs at different points in time. Ice shelves are indicated in light grey.

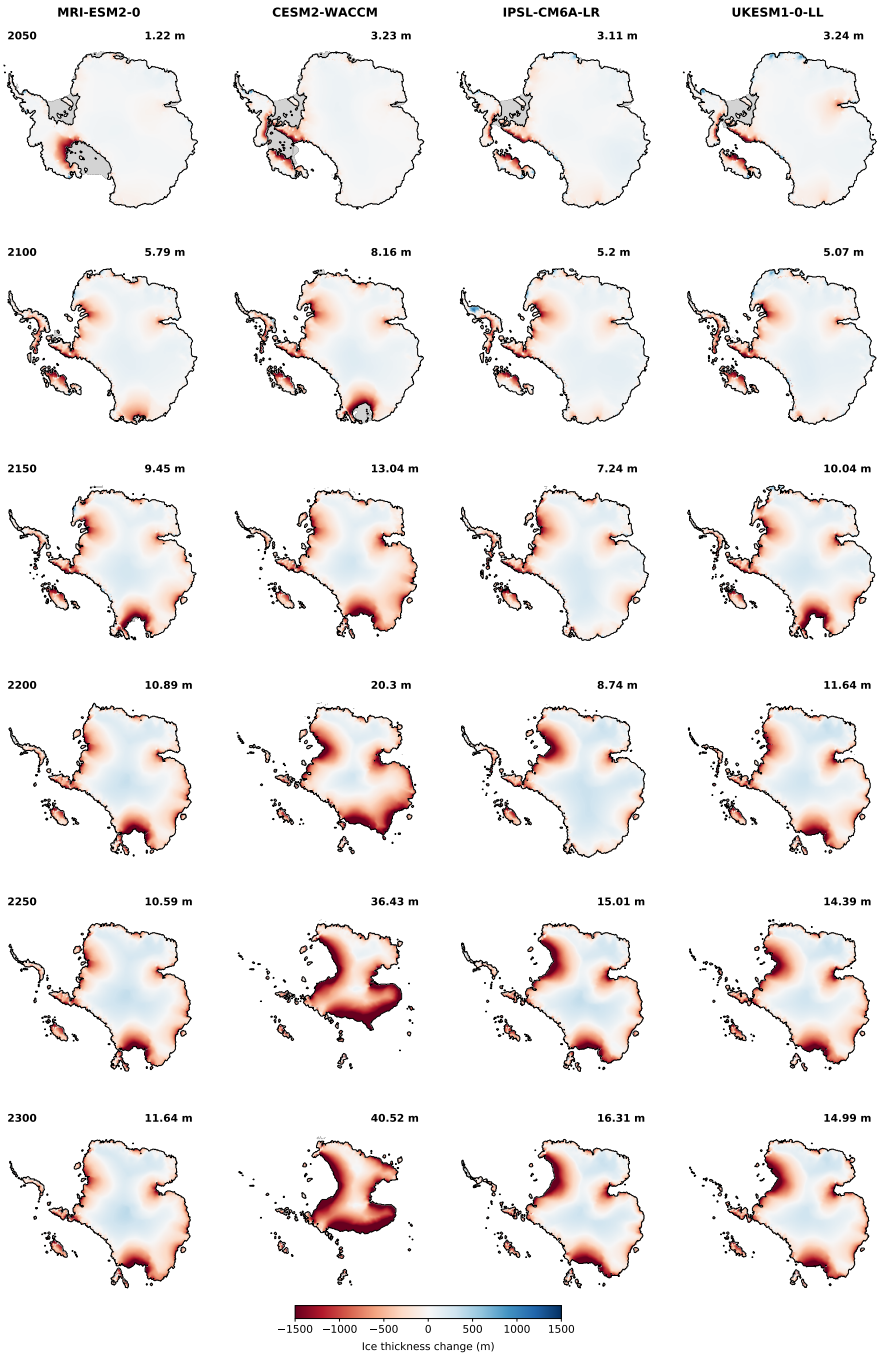

Figure S18. Committed ice–sheet configuration as determined by PISM following the higher–emission pathway SSP5-8.5 and using an atmospheric climatology based on MAR. Shown is the committed thickness change and grounding–line location (marked in black) in year 7000 when stabilising climatic boundary conditions as projected by CMIP6 GCMs at different points in time. Ice shelves are indicated in light grey.

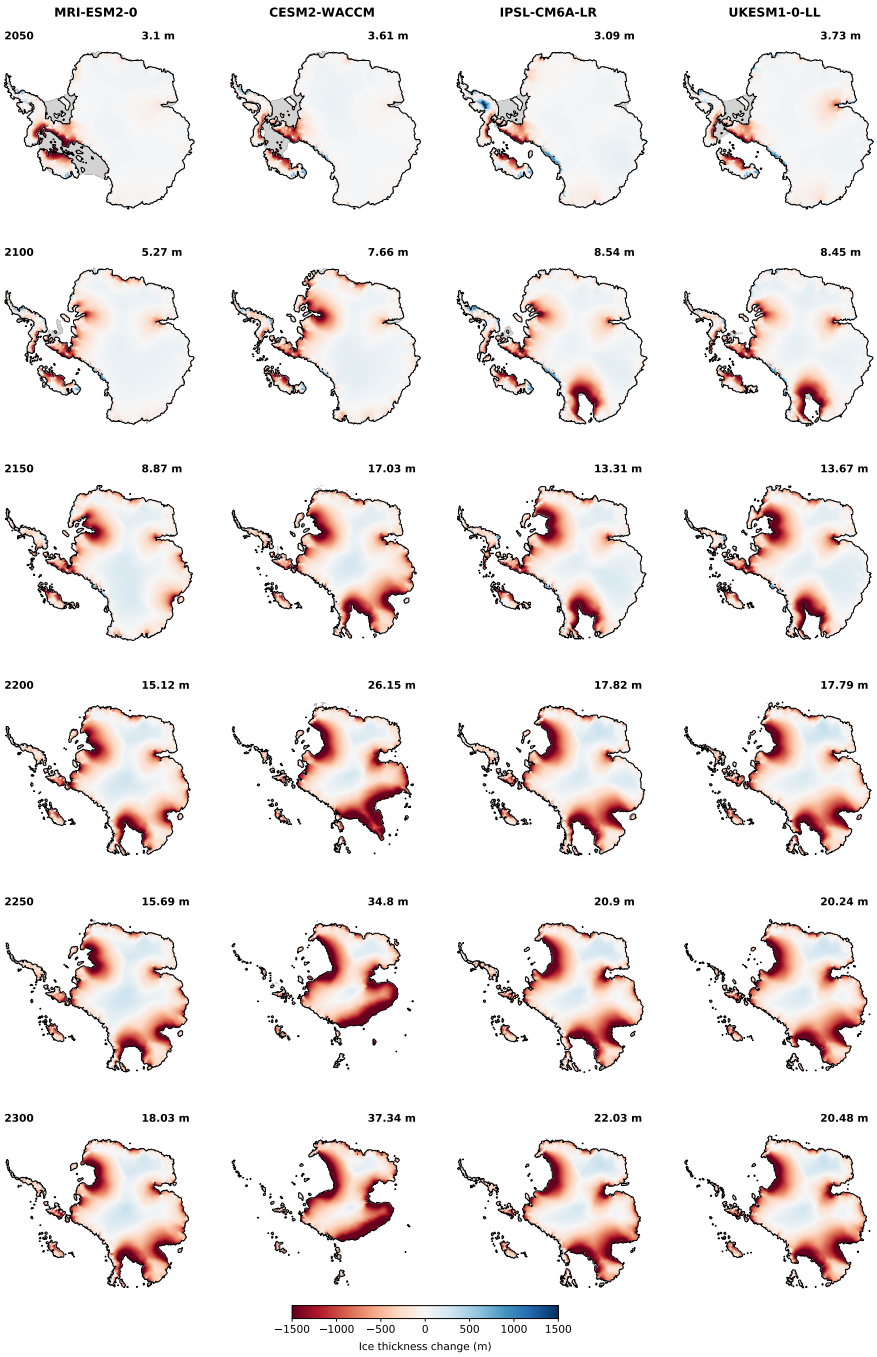

Figure S19. Committed ice–sheet configuration as determined by PISM following the higher–emission pathway SSP5-8.5 and using an atmospheric climatology based on RACMO. Shown is the committed thickness change and grounding–line location (marked in black) in year 7000 when stabilising climatic boundary conditions as projected by CMIP6 GCMs at different points in time. Ice shelves are indicated in light grey.

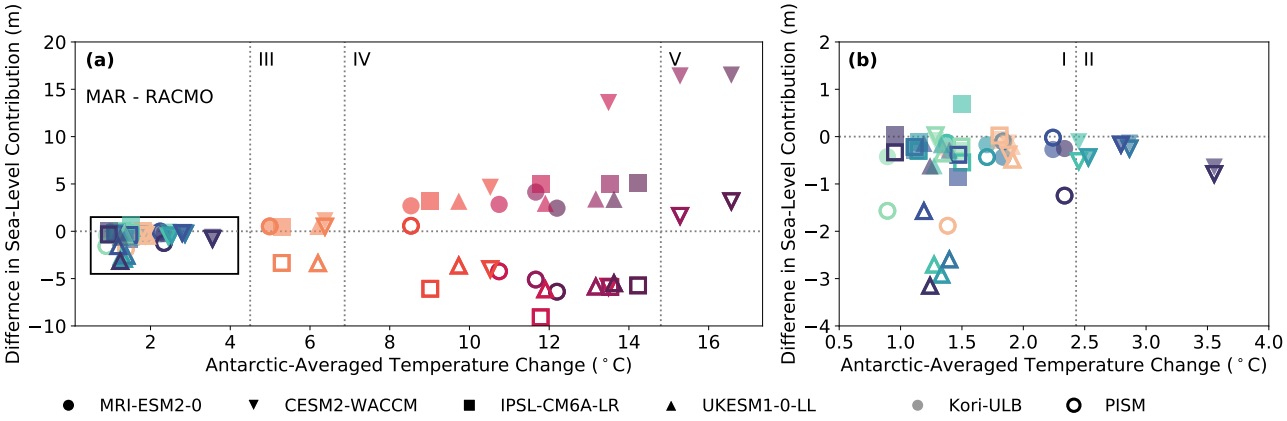

Figure S20. Intra–model difference in committed sea–level contribution from the Antarctic Ice Sheet. Difference in long–term ice loss from the Antarctic Ice Sheet (in meters sea–level equivalent) for year 7000 in response to Antarctic–averaged atmospheric temperature change (compared to 1995–2014) between distinct initial states using an atmospheric climatology based on MAR and RACMO in Kori-ULB and PISM. The change in climatic boundary conditions is sustained for several millennia. (b) is a zoom into (a) for a lower atmospheric temperature change.

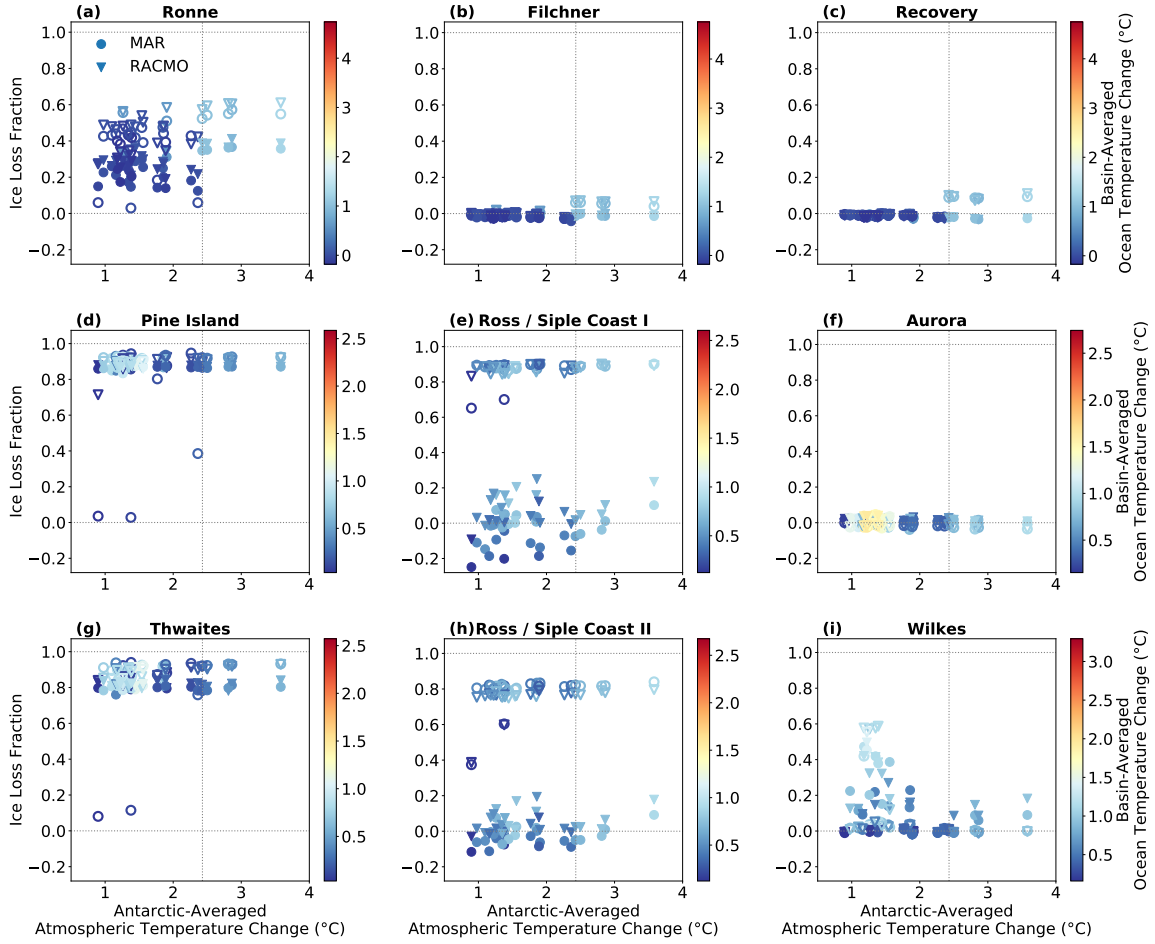

Figure S21. Ice loss from Antarctic drainage basins Long–term ice loss from different Antarctic drainage basins (as fraction of respective sea–level rise potential) for the year 7000 in response to Antarctic–averaged atmospheric temperature change (compared to 1995–2014). The basin–averaged oceanic temperature change is represented by the colouring. This is a zoom–in to Figure 5.